



Characterization of Hydrolysis Lignin Bonding Properties During the Pelletization of Eucalyptus Sawdust

Weizhen Li^{1,2,3} · Yang Jiang^{1,2,3} · Xiuli Yin^{1,2,3}

Received: 25 December 2017 / Accepted: 22 August 2018 / Published online: 18 September 2018
© Springer Nature B.V. 2018

Abstract

This work assessed the effects of the bonding of hydrolysis lignin during the pelletization of eucalyptus sawdust. The characteristic thermal transition temperatures of hydrolysis lignin and eucalyptus sawdust were initially determined using differential scanning calorimetry, and the glass transition temperatures (T_g) were recorded at 94.4 and 87 °C, respectively, while their melting temperatures were recorded at 136.5 and 127.4 °C, respectively. The temperature range of 80–160 °C is set in order to include the thermal transition temperature spans of these materials. Single pellet making experiments were conducted using a uniaxial piston–cylinder compression apparatus and acceptable pellet properties were observed when pelletizing at temperatures between the end point of the T_g region and the melting temperature and at 20–30% hydrolysis lignin content. Examinations of the internal cross-sections of these pellets by scanning electron microscopy showed that cracks between particles were filled sufficiently with hydrolysis lignin, allowing particles adhere to one another tightly after the glass transition of hydrolysis lignin. The assessment of functional group changes during the pelletization process using FTIR found that the lignin evidently improves the physical properties of the pellets by reducing the quantity of some oxygen-containing functional groups while elevating the concentrations of alcohol or phenol –OH groups, hydrocarbon or naphthene –CH bonds.

Keywords Eucalyptus sawdust pelletization · Hydrolysis lignin · Glass transition temperature · Bonding · Functional group

Statement of Novelty

The bonding function of hydrolysis lignin during the pelletization of eucalyptus sawdust was examined in this work. The results found that acceptable pellet properties were observed when pelletizing at temperatures between the end point of the T_g region and the melting temperature and at 20–30% hydrolysis lignin content. In this condition cracks between particles were filled sufficiently with hydrolysis lignin, allowing particles adhere to one another tightly. The reasons that hydrolysis lignin can evidently improves the physical

properties of the pellets are the reduction of some oxygen-containing functional groups and the elevation of alcohol or phenol –OH groups, hydrocarbon or naphthene –CH bonds.

Introduction

The process of converting various types of non-shaped agricultural and forest residues into shaped pellets under a certain temperature and pressure is biomass pelletization technology. The technology can enhance the physical properties of biomass and produce uniform, clean, stable, and energy denser biomass for environment-friendly fuels production [1]. The biomass pellets considered as a convenient option for easily handled, stored, and transported long distances, thus biomass pellets are being used in huge quantity widely in many fields such as power plants, heating, biochemical or thermochemical conversion etc. [2].

In the pelletization process the components such as lignin, protein, starch and watersoluble carbohydrates are natural binders in biomass materials [3–5]. When the temperature is increased the lignin component becomes softened

✉ Yang Jiang
jiangyang@ms.giec.ac.cn

¹ Guangzhou Institute of Energy Conversion, Chinese Academy of Sciences, No.2, Nengyuan Rd, Wushan, Tianhe District, Guangzhou 510640, China

² CAS Key Laboratory of Renewable Energy, Guangzhou 510640, China

³ Guangdong Provincial Key Laboratory of New and Renewable Energy Research and Development, Guangzhou 510640, China

which then acts as a natural binder. Once pellets are cooled down, the shape and hardness of pellets retained and thus the pellets formed. As a natural binder, lignin plays a key role in bonding during the biomass pelletization process based on its thermal transition characteristics. Lignin shifts from softening to melting as its viscosity enhance with increasing temperature [6]. The lignin subsequently bind with cellulose, hemicellulose and other biomass components in response to the application of pressure. Therefore, both temperature and lignin content are the main factors influencing the extent of bonding.

Stelte et al. studied the effect of the lignin glass transition on the pelletizing properties of wheat straw. This prior study applied pelletizing temperatures both above and below the glass transition temperature (T_g) of lignin and assessed the compression strength, density and fracture surfaces of the resulting pellets. Pellets pressed at 30 °C (below the lignin T_g) were found to have a lower density and reduced compression strength as well as a tendency to expand in length after the pelletizing process compared with pellets pressed at 100 °C (above the T_g) [7]. Dam et al. reported that various product quality indicators were improved when the original lignin in the plant tissues becomes molten during processing [8]. Castellano et al. concluded that the composition of the raw material was the most important parameter affecting the quality and properties of the pellets. Pellets obtained from lower extractives with higher lignin contents (that is, woody materials) exhibited improved physical properties. Woody particles were found to more readily deform when pelletized, while herbaceous materials preserved their original shape [9]. Lehtikangas et al. tested pellets made from fresh and stored sawdust, bark and logging residues (a mixture of Norway spruce and Scots pine) and found that pellet density had no effect on durability, in contrast to the lignin content, which exhibited a positive correlation with density [10]. Whereas, Wilson concluded that lignin content in hardwoods and softwoods had no impact on pellet durability [11]. Bradfield et al. stated that optimized lignin concentrations can lead to bonding between the crystal structures in the wood polymers. Lignin proportions above this critical value can cause the accumulation of excess lignin, which in turn lowers the strength and durability of the pellets because of the poor internal strength of the lignin itself [12].

Together, these studies suggest that the function of lignin will vary depending on the materials being pelletized and

did not submit the optimal pelletization temperature region. The main purpose of the present work was therefore to examine the bonding function of *hydrolysis lignin* (HL) during the *eucalyptus sawdust* (ES) pelletization process. Single pellet making experiments were conducted using a uniaxial piston–cylinder compression apparatus. The effects of temperature and the HL content on pellet properties were studied in detail based on analysis of the product thermal transition temperatures by differential scanning calorimetry (DSC). Scanning electron microscopy (SEM) was also used to examine the internal morphology of the pellets and Fourier transform infrared (FTIR) spectroscopy was used to analyze functional group changes during the pelletization process.

Materials and Methods

Materials

ES (*Eucalyptus urophylla*, a representative of fast-growing woods) was chosen as a raw material considering the disposal of millions of tons of wastes from the processing and utilization of eucalyptus in South China. ES was obtained from a wood processing factory in Yangshan County, Guangdong province, China. HL, which is discarded as wastes and can be obtained easily, is a by-product in the process of preparing aviation fuel from biomass. The HL can be easily promoted for industrial production in the process of biomass pelletization because the HL can be treated as an industrial grade lignin, which is easy to obtain. Hence, HL (the hydrolysis product of corn stover) was used as a representative of lignin in the present work. The sample of HL was acquired from the Guangzhou Institute of Energy Conversion, Chinese Academy of Sciences. Table 1 shows the properties of these raw materials. The moisture content, volatile matter, fixed carbon, and ash content were measured by a proximate analyzer (5E-MACIV, Changsha Kaiyuan Instruments Co., Ltd., China). The elemental composition was determined by an elemental analyzer (Vario EL CHNS, Elementar Analysensysteme GmbH, Germany). The higher heating value (HHV) was measured by microcomputer calorimeter (WZR-1T-CII, Changsha Bente Instrument, China). The chemical composition was determined according to the standard established by National Renewable Energy

Table 1 Ultimate and proximate analysis data and HHV for ES and HL

Materials	Ultimate analysis (%)				Proximate analysis (%)				Chemical composition (%)				HHV (kJ/kg)
	C	H	N	S	M_{ad}	A_{ad}	V_{ad}	FC_{ad}	Cellulose	Hemicelluloses	Lignin	Extractives	
ES	44.23	6.12	0.13	0	11.04	1.48	82.04	5.45	39.58	21.53	35.04	2.37	16,964
HL	47.31	5.50	0.19	0.34	3.70	8.86	63.92	23.53	9.67	4.18	74.01	3.28	19,049

Laboratory [13, 14]. These raw materials were pulverized and sieved to obtain particles with diameters between 2 and 3 mm. The ground materials were subsequently dried in an oven at 105 °C until a stable mass was obtained. The moisture mass content of each dry ground raw material was adjusted to approximately 12% by adding a predetermined amount of deionized water using a spray bottle followed by storage in an airtight plastic box for 1 week [15].

Methods

DSC

Li examined three industrial unannealed lignin samples using DSC and found that they generated broad endothermic peaks due to water vaporization that prevented accurate determination of the T_g [16]. Therefore, sub- T_g annealing was required to vaporize water in the samples as well as to remove the thermal history of the lignin. Because lignin will undergo heat-promoted reactions at approximately 120 °C, annealing at 90 °C should be employed for this purpose.

In the present work, the thermal transition characteristics of ES and HL were assessed using a DSC instrument (Q200, TA Instruments, Inc. America) equipped with a cooling device. Samples were initially preheated to remove residual moisture, at a temperature sufficiently low so as to avoid thermal decomposition of the lignin and other constituents. The samples (6–8 mg after drying) were then rapidly cooled to eliminate any effects of the preheating history and subsequently reheated based on set temperature programming. The specific temperature program was as follows: heating to 90 °C for 10 min, cooling to 0 °C for approximately 3 min, and heating to 200 °C at 10 °C. The data generated during the final heating process was used for DSC analysis. The samples were held under a 25 ml/min flow of N_2 throughout each process [17].

Biomass Compression Procedure

The single pellet densification experiments were conducted using a uniaxial piston–cylinder compression apparatus (WD-100KE, Grandtry Testing Instruments Co, Ltd., China). The compression cylinder used for this study had an inner diameter of 10.2 mm and a universal testing machine with a compression rod having a diameter of 10 mm was used to apply pressure. The instrument was controlled using a computer in conjunction with the TestWorks software package. In each trial, the apparatus was first equilibrated at the desired temperature using a heating coil, thermocouple and temperature control unit, after which a known mass of raw material was transferred into the cylinder and compression was initiated. As a result, a pellet was extruded from the cylinder. The compression parameters included a rate of

20 mm/min, a maximum force of 6000 N, and a maximum force hold time of 40 s [18, 19]. Force and displacement data during compression of the ES were obtained automatically by TestWorks software.

The recorded force and displacement data during pelletization was applied for calculating the energy consumption associated with compaction by integrating the force versus displacement curves. The specific energy consumption (SEC) was determined using the Eq. (1) [20].

$$SEC = W/m = \int f \times ds/m \tag{1}$$

where W, m, f, and s are the energy consumption in J, pellet mass in kg, force in kN, and rod displacement in mm.

After ejection from the cylinder the pellets were stored in a sealed bag for 2 weeks, then the mass and the volume of an individual pellet was obtained using a scale and measurements with a Vernier micrometer. The density (Herein, the density is the relaxed density RDS) of each pellet was calculated from the results of these measurements using the Eq. (2) [21].

$$RDS = 4m/\pi d^2l \tag{2}$$

where m, d and l are the mass in kg, the diameter in m and the length in m.

Subsequently, the Meyer hardness (H_M) of each pellet was obtained using the universal testing machine. A single pellet was positioned on a flat horizontal surface, then a 7 mm diameter compression rod, which was fixed on the universal testing machine, with the hemispherical top vertically moved downward at a speed of 5 mm/min. Both the force and displacement of the compression rod were recorded by the universal testing machine TestWorks software. The H_M value was calculated using the Eq. (3) [22, 23].

$$H_M = \frac{F}{\pi \sqrt{D \times h - h^2} \sqrt{\frac{D_p^2}{4} - \left[\frac{\frac{D_p^2}{2} + \frac{D \times D_p}{2} - D \times h - D_p \times h + h^2}{D + D_p - 2h} \right]}} \tag{3}$$

where F is the force required to break the pellet in N, D is the compression rod diameter of 7 mm, h is the indentation depth corresponding to the piston displacement before the pellet breakage in mm, and D_p is the pellet diameter of 10 mm.

During the biomass compression procedure each trial was repeated five times and every time the result of RDS was acquired. The final results reported in the present work were the average of the three middle results, and then the H_M and SEC average results corresponding to the RDS three middle results were determined and reported.

The HHV of the pellets produced with varying HL content 10–40% can be determined by the Eq. (4).

$$\text{HHV}_{\text{Pellet}} = \text{HHV}_{\text{ES}} \times \text{ES}\% + \text{HHV}_{\text{HL}} \times \text{HL}\% \quad (4)$$

where HHV_{ES} is 16,964 kJ/kg, HHV_{HL} is 19,049 kJ/kg, ES% is mass percent of ES in the pellet, HL% is mass percent of HL in the pellet, and $\text{ES}\% + \text{HL}\% = 100\%$.

SEM

The micromorphology of each pellet was analyzed using SEM (Hitachi S-4800, Hitachi, Ltd., Japan). A thin layer in each pellet was cut off from the fractured surface formed during the H_M test process using a razor blade. Care was taken to obtain the samples with internal cross-sections. In preparation for observations, each sample was attached to a metal post with conductive carbon tape and the upper surface was coated with a thin layer of gold. Images of pellet internal cross-sections were acquired at various magnifications, operating at a 2 kV acceleration voltage. A back-scattered electron detector was used for image analysis.

FTIR

FTIR spectra (VERTEX70, Bruker Corporation, Germany) were obtained to assess functional group changes during the pelletization process. The ground samples and KBr were dried in an oven at 105 °C to constant weight, then each dry, ground sample (2 mg) was mixed with KBr (200 mg). The mixture was grinded in a mortar to a diameter of about 2 µm under an infrared lamp. The grinded mixture was pressed into a 0.1–1.0 mm tablet that was subsequently presented to the spectrometer. All spectra were recorded over the range of 4000–400 cm^{-1} .

Results and Discussion

Thermal Transition Characteristic Temperatures

The DSC curves obtained from the ES and HL are shown in Fig. 1. The initial endothermic events indicate the T_g regions of each material while the second endothermic peaks are associated with melting [24]. The T_g and melting temperatures determined from these plots are summarized in Table 2.

The data in Table 2 demonstrate that the T_g and melting temperature of HL were both higher than those of the ES. Below 84.4 °C, the glass transition of the HL does not occur. Between 84.4 and 104.3 °C, the glass transition of the HL occurs gradually and with further increases to 136.5 °C, the melting of the HL occurs. Therefore, the temperature parameter was set in the range of 80–160 °C, including the thermal transition temperature spans of both HL and ES, so as to the HL can acts as a binder.

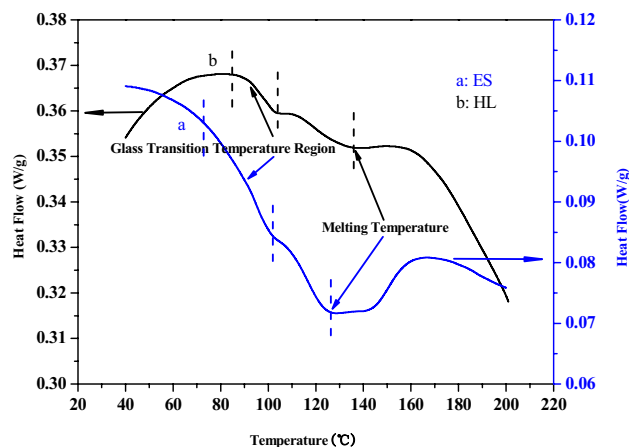


Fig. 1 The DSC curves obtained from ES and HL

Table 2 Thermal transition temperatures determined for ES and HL

Samples	Glass transition temperature region (°C)			Melting temperature (T_m)
	Onset	Mid-point (T_g)	End point	
ES	72	87	102	127.4
HL	84.4	94.4	104.3	136.5

$$T_g = (T_{\text{end point}} + T_{\text{onset}})/2 \text{ in the } T_g \text{ region}$$

Pellets Physical Properties

Figure 2 presents the photographic images of pellets produced under varying conditions. The HHV of the pellets with varying HL content 10–40% calculated results respectively are 17,173, 17,381, 17,590, 17,798 kJ/kg. These showed the increase of HL adding amount is beneficial for the pellets in terms of HHV.

Figure 3 provides the plots of RDS, H_M and SEC values as functions of HL content at various processing temperatures. The RDS (Fig. 3a) evidently monotonically increased with HL content at a given temperature. For instance, the RDS increased from 813.16 to 1016.68 kg/m^3 with HL content increasing from 0 to 40% at the given temperature of 100 °C. RDS values also increased with the raising temperature at a constant HL content. Experimental values indicated that RDS increased from 755.11 to 1167.68 kg/m^3 with temperature increasing from 80 to 160 °C at the given HL content of 30%. These indicate that the increase of HL content and temperature are beneficial for the pellets in terms of RDS. However, the rate of increase in the RDS was more rapid at temperatures below 120 °C than temperatures above 120 °C at a constant HL content. As an instance, the RDS increased from 635.51 to 1017.30 and finally 1119.46 kg/m^3 , respectively corresponding to 60.08%, 10.04% increase rate, at 80, 120 and 160 °C at a constant lignin content of

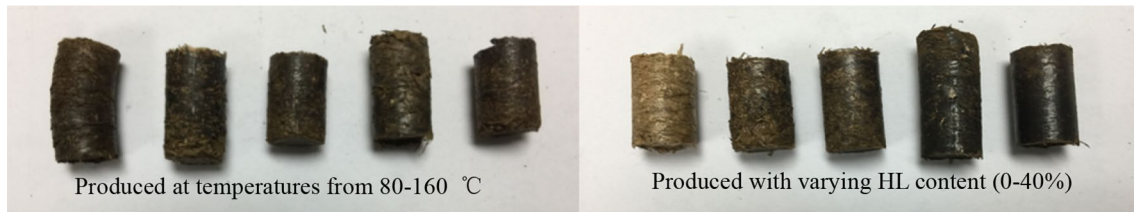


Fig. 2 Photographic images of pellet specimens

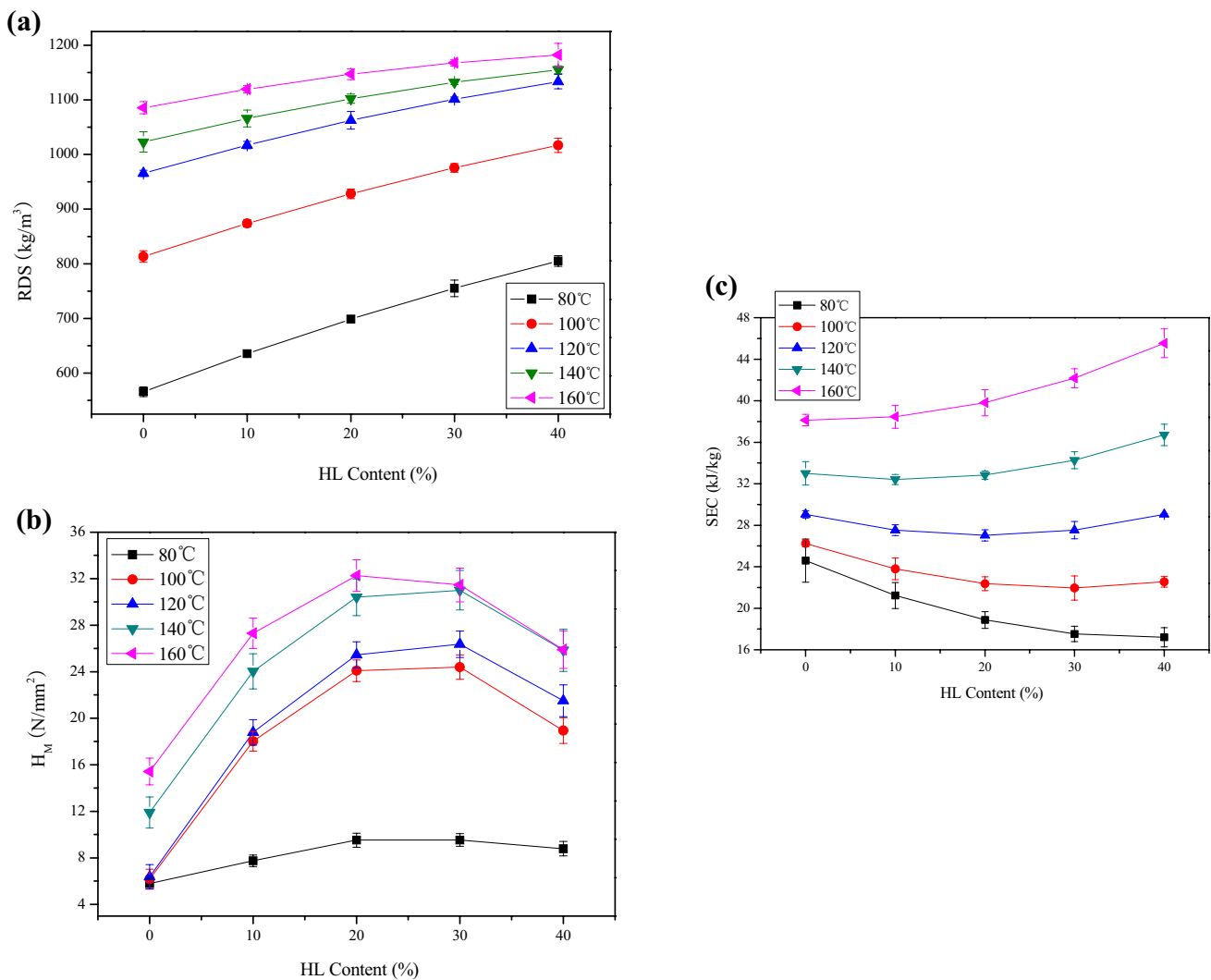


Fig. 3 Effects of the HL concentration and processing temperature on **a** RDS, **b** H_M , and **c** SEC values

10%. These results are in agreement with the DSC data. As the temperature was raised within the T_g region between 80 and 120 °C, the HL viscosity increased rapidly, leading to a rapid improvement in pellet RDS. Approaching the melting temperature above 120 °C, the HL viscosity gradually reached a maximum, the pellet RDS was improved more gradually [25]. These results demonstrate that the optimal

processing temperature is between the end of the T_g region and the melting temperature.

The H_M values (Fig. 3b) initially increase and then decrease as the HL level is raised while maintaining a constant temperature [26]. The maximum H_M appears in the range of 20–30% HL content. Experimental values showed that H_M increases from 6.19 to 24.40 N/mm² and then

drops to 18.94 N/mm² at HL concentrations of 0, 30, 40%, respectively, while maintaining the constant temperature of 100 °C. This shows the increasing of HL content in the range of 20–30% promotes the H_M of pellets maximally. H_M also increased along with the processing temperature at a constant lignin level. An instance is the increase in H_M from 9.52 to 32.26 N/mm² on temperature going from 80 to 160 °C at 20% lignin. The increase of temperature is also beneficial for the pellets in terms of H_M .

The SEC values (Fig. 3c) demonstrate different changes with the increasing content of HL at a constant temperature. At 80 °C, the SEC values monotonically decreased from 24.60 to 17.20 kJ/kg as the HL level was raised from 0 to 40%. In the temperature range of 100–140 °C, the SEC values initially decreased and then increased as the HL level was raised from 0 to 40%. For instance, SEC decreased from 33.01 to 32.41 kJ/kg and then lifted to 36.71 kJ/kg at the HL concentrations of 0, 10%, 40%, respectively, while maintaining the constant temperature of 140 °C. At 160 °C, the SEC values monotonically increased from 38.13 to 45.53 kJ/kg as the HL level was raised from 0 to 40%. These data indicate the SEC can be reduced by adding HL, but the reduction effects would be weakened by the higher temperatures [27]. Apparently, SEC values gradually increase with raising temperature at a specific HL level and the corresponding increase rates became rapid gradually [28]. For instance, over the 20 °C intervals as the temperature is raised from 80 to 160 °C at 10% HL content, the SEC values are 21.23 kJ/kg, 23.80 kJ/kg, 27.53 kJ/kg, 32.41 kJ/kg, 38.46 kJ/kg, corresponding increase rates are 12.10%, 15.67%, 17.76%, 18.66% respectively.

These results demonstrate that the increases of HL content within a certain range is beneficial for pellets associate with HHV, RDS, H_M , SEC at a given temperature, and the raise of temperature can improve the RDS, H_M of pellets when maintaining a HL content. With appropriate adding amount and temperature, the viscosity of HL could reach in maximum, and enhanced the bonding of HL. In contrast, an excess of lignin make the compression process more difficult resulting in lower H_M of pellets and more SEC

during pelletization process. On the whole, pellets produced with HL content between 20% and 30% at the temperature between the end of the T_g region and the melting temperature have the relatively higher RDS, higher H_M , lower SEC, and thus the HL adding amount 20–30% and the temperature range of 120–140 °C can be recommended during ES pelletization process.

HL Bonding Effects

Temperature

SEM images of internal cross-sections of pellets produced at 80, 120 and 160 °C, respectively, using 20% HL content are shown in Fig. 4. Figure 4a indicates that, below the onset of glass transition temperature region of HL, particles were filled with cracks that could result in particle loose associations with each other. The regions outlined by red borders in Fig. 4b, c demonstrate the glass transition of HL. The higher temperature between the end of the T_g region and the melting temperature increased the viscosity of HL, allowing particles adhere to one another tightly [29]. The particle connections in Fig. 4b, c are very similar, indicating that when the temperature is above T_g , further raising the temperature did not improve any significant changes in agreement with the DSC results and pellet physical properties data.

HL Content

SEM images of pellet internal cross-sections made at temperature of 120 °C using 0%, 20%, and 40% HL content, respectively, are presented in Fig. 5. The image in Fig. 5a demonstrate that the pellets made without HL have poor particle adhesion without any filling agent in the cracks. In contrast, the particles in Fig. 5b have a more orderly arrangement with sufficient filling agent in the cracks, while the particle surfaces and cracks in Fig. 5c exhibit the accumulation of excess HL. These images confirm that the bonding of HL between particles can be enhanced at appropriate content. but that too much HL content could lead to accumulation

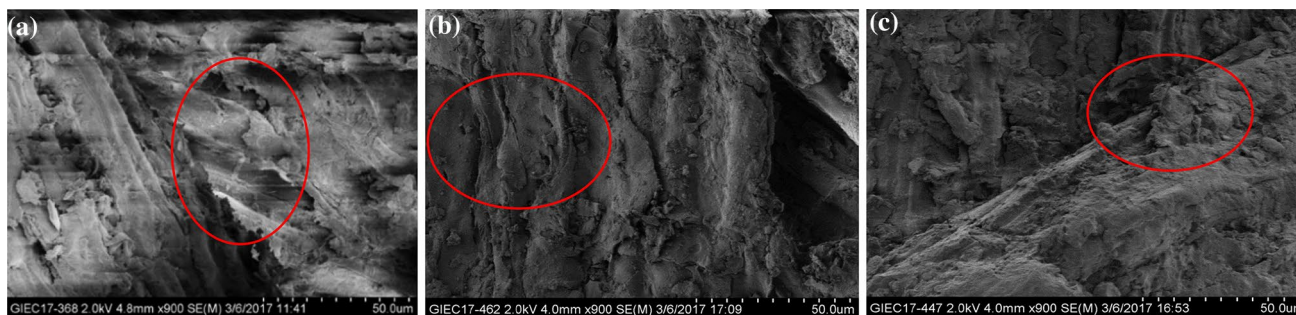


Fig. 4 SEM images of pellet internal cross-sections produced at **a** 80, **b** 120, and **c** 160 °C using 20% HL content

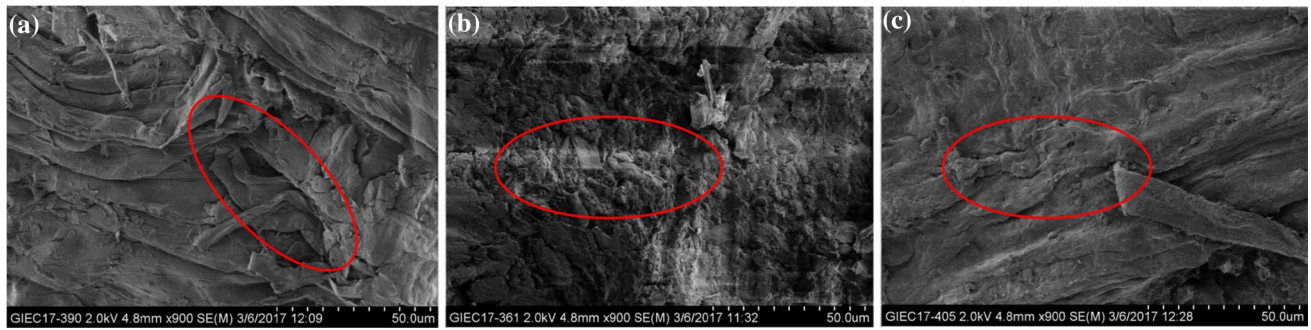


Fig. 5 SEM images of pellet internal cross-sections produced using **a** 0%, **b** 20%, and **c** 40% HL content at temperature of 120 °C

that weakens the bonding effect [30, 31]. These findings are also consistent with the pellet properties data.

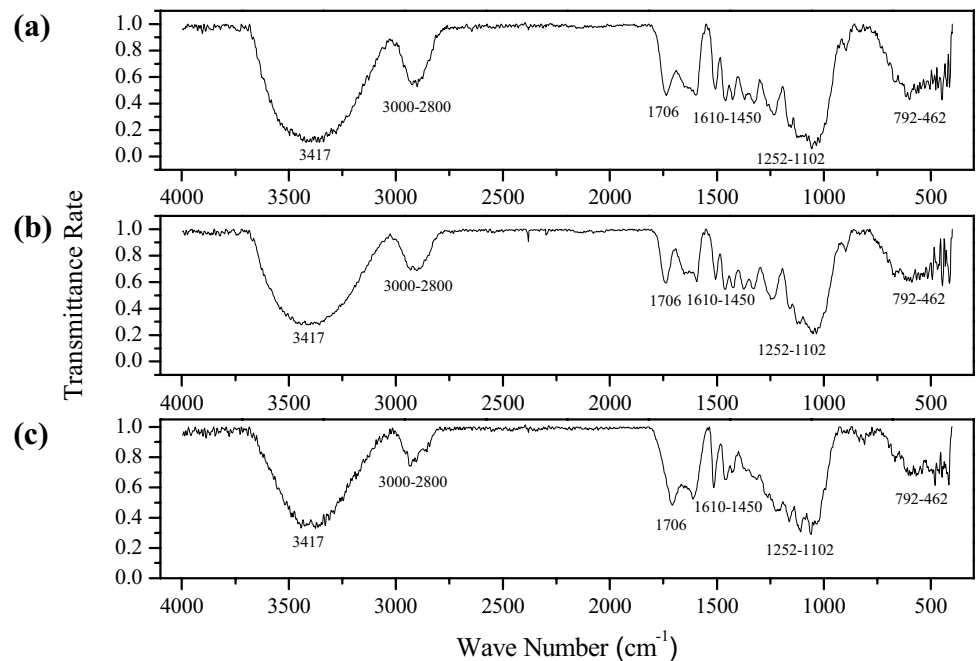
Functional Groups Change

The FTIR spectra of the products are shown in Fig. 6. As can be seen, the locations of all sample characteristic peaks are essentially the same in each case, but the peak heights and areas are different, indicating that although the functional groups in all sample are the same, their concentrations are different.

The characteristic peaks primarily distribute in the waves of 3600–3000, 3000–2800, 1800–1000 and 462–792 cm^{-1} . The first wave range of 3600–3000 cm^{-1} corresponds to vibrations and absorptions of hydroxyl –OH group that can form various hydrogen bonds. The peak at 3419 cm^{-1} is attributed to the stretching vibrations of alcohol and phenol

–OH groups. It is evident that all three samples contain these groups and that the –OH group content is in the order of HL > the ES pellet with 20% HL content > the ES pellet based on the converse transmittance rate. This result shows that the HL addition increases the –OH group concentration in the pellets. The wave 3000–2800 cm^{-1} range corresponds to the absorption and vibration of hydroxyl C–H bonds, which are mainly caused by the symmetric and asymmetric stretching vibration of fatty hydrocarbon or naphthene –CH₃ and –CH₂ groups. The hydroxyl content is HL > the ES pellet with 20% HL content > the ES pellet, apparently because of the sample converse transmission rate. That is to say the HL adding lead to C–H bonds in the pellets. The region of 1800–1000 cm^{-1} is associated with functional groups containing oxygen. Specifically, the 1706 cm^{-1} is attributed to stretching vibration of carboxyl C=O bonds, the 1610–1450 cm^{-1} region corresponds to benzene or

Fig. 6 The FTIR spectra of three test specimens **a** HL, **b** a ES pellet with 20% HL content, **c** a ES pellet



aromatic rings, and the 1252–1102 cm^{-1} region is attributed to stretching vibration of phenol, alcohol, ether, $-\text{C}=\text{O}$, $-\text{C}=\text{C}$ or $-\text{OH}$ groups. The 1706 and 1252–1102 cm^{-1} peak intensities generated by sample 2 were lower than those of samples 1 and 3. These illustrate that the addition of HL led to bond rupture and reduced the concentration of these oxygen containing functional groups. The 792–462 cm^{-1} region corresponds to bending vibrations of aromatic $-\text{CH}$ bonds, and the $-\text{CH}$ content in this range is in the order of $\text{HL} > \text{ES}$ pellet with 20% HL content $>$ the ES pellet.

These FTIR results show that the addition of HL ruptured and reduced the concentration of certain oxygen-containing functional groups while increasing the concentrations of $-\text{OH}$ groups and $-\text{CH}$ bonds, so as to improve the pellet properties. This conclusion is in agreement with the data previously published by Stelte and Li H [15, 28].

Conclusions

The pellets produced with varying HL content 0–40% at temperatures from 80 to 160 °C physical property analytical results indicated that the increases of HL content within a certain range is beneficial for pellets in terms of HHV, RDS, H_M , SEC at a given temperature, and the raise of temperature can improve the RDS, H_M of pellets while maintaining a HL content. The pellets made using 20–30% HL content and temperature of 120–140 °C, which locates between the end of the T_g region and the melting temperature, were found to have the relatively higher RDS, higher H_M and lower SEC. SEM images of internal cross-sections of these pellets showed that the particles have a more orderly arrangement with sufficient HL filling in the cracks, confirming that the appropriate lignin content and temperature range can enhance the bonding between particles. The explanations of pellet property improvement by adding HL based on FTIR results are the $-\text{OH}$ groups and $-\text{CH}$ bonds concentration increase in pellets.

Acknowledgements This work was supported by the National Natural Science Foundation of China (51661145022), Guangdong Provincial Natural Science Foundation Project (2017B030308002), Heilongjiang Science and Technology Planning Project, Chinese Academy of Sciences Key Laboratory of Renewable Energy (y807j91001).

References

1. Ståhl, M., Berghel, J.: Energy efficient pilot-scale production of wood fuel pellets made from a raw material mix including sawdust and rapeseed cake. *Biomass Bioenergy* **35**(12), 4849–4854 (2011)
2. Kim, S., Dale, B.E.: Global potential bioethanol production from wasted crops and crop residues. *Biomass Bioenergy* **26**(4), 361–375 (2004)
3. Kaliyan, N., Morey, R.V.: Factors affecting strength and durability of densified biomass products. *Biomass Bioenergy* **33**(3), 337–359 (2009)
4. Tabil, L.G.: *Pelleting and Binding Characteristics of Alfalfa*. University of Saskatchewan, Saskatoon (1996)
5. Cavalcanti, W.B.: The Effect of Ingredient Composition on the Physical Quality of Pelleted Feeds: A Mixture Experimental Approach. Kansas State University, Kansas (2004)
6. Nielsen, N.P.K., Gardner, D.J., Felby, C.: Effect of extractives and storage on the pelletizing process of sawdust. *Fuel* **89**(1), 94–98 (2010)
7. Stelte, W., Clemons, C., Holm, J.K., Ahrenfeldt, J., Henriksen, U.B., Sanadi, A.R.: Fuel pellets from wheat straw: the effect of lignin glass transition and surface waxes on pelletizing properties. *Bioenergy Res.* **5**(2), 450–458 (2012)
8. van Dam, J.E.G., van den Oever, M.J.A., Teunissen, W., Keijsers, E.R.P., Peralta, A.G.: Process for production of high density/high performance binderless boards from whole coconut husk: part 1: lignin as intrinsic thermosetting binder resin. *Ind. Crops Prod.* **19**(3), 207–216 (2004)
9. Castellano, J.M., Gómez, M., Fernández, M., Esteban, L.S., Carrasco, J.E.: Study on the effects of raw materials composition and pelletization conditions on the quality and properties of pellets obtained from different woody and non woody biomasses. *Fuel* **139**, 629–636 (2015)
10. Lehtikangas, P.: Quality properties of pelletised sawdust, logging residues and bark. *Biomass Bioenergy* **20**(5), 351–360 (2001)
11. Wilson, T.O.: *Factors Affecting the Wood Pellet Durability*. Pennsylvania State University, State College (2010)
12. Bradfield, J., Levi, M.P.: Effect of species and wood to bark ratio on pelleting of southern woods. *For. Prod. J.* **34**(1), 61–63 (1984)
13. Sluiter, A., Ruiz, R., Scarlata, C., Sluiter, J., Templeton, D.: Determination of Extractives in Biomass. NREL National Renewable Energy Laboratory-NREL/TP-510-42619. NREL Laboratory Analytical Procedure (LAP), Colorado (2005)
14. Sluiter, A., Hames, B., Ruiz, R., Scarlata, C., Sluiter, J., Templeton, D., Crocker, D.: Determination of Structural Carbohydrates and Lignin in Biomass. NREL National Renewable Energy Laboratory-NREL/TP-510-42618. Laboratory Analytical Procedure (LAP), Colorado (2011)
15. Stelte, W., Holm, J.K., Sanadi, A.R., Barsberg, S., Ahrenfeldt, J., Henriksen, U.B.: A study of bonding and failure mechanisms in fuel pellets from different biomass resources. *Biomass Bioenergy* **35**(2), 910–918 (2011)
16. Li, H., McDonald, A.G.: Fractionation and characterization of industrial lignins. *Ind. Crops Prod.* **62**, 67–76 (2014)
17. Poursorkhabi, V., Misra, M., Mohanty, A.K.: Extraction of lignin from a coproduct of the cellulosic ethanol industry and its thermal characterization. *BioResources* **8**(4), 5083–5101 (2013)
18. Kaliyan, N., Morey, R.V.: Constitutive model for densification of corn stover and switchgrass. *Biosyst. Eng.* **104**(1), 47–63 (2009)
19. Wang, G.L., Jiang, Y., Li, W.Z., Yin, X.L.: Process optimization of corn stover compression molding experiments based on response surface method. *Trans. Chin. Soc. Agric. Eng.* **32**(13), 223–227 (2016)
20. Li, H., Jiang, L.B., Li, C.Z., Liang, J., Yuan, X.Z., Xiao, Z.H., Xiao, Z.H., Wang, H.: Co-pelletization of sewage sludge and biomass: the energy input and properties of pellets. *Fuel Process. Technol.* **132**, 55–61 (2015)
21. Liu, Z.J., Liu, X.G., Fei, B.H., Jiang, Z.H., Cai, Z.Y., Yu, Y.: The properties of pellets from mixing bamboo and rice straw. *Renew. Energy* **55**(4), 1–5 (2013)
22. Peng, J.H., Bi, H.T., Lim, C.J., Sokhansanj, S.: Study on density, hardness, and moisture uptake of torrefied wood pellets. *Energy Fuels* **27**(2), 967–974 (2013)

23. Peng, J.H., Wang, J.S., Bi, X.T., Lim, C.J., Sokhansanj, S., Peng, H.C., Jia, D.N.: Effects of thermal treatment on energy density and hardness of torrefied wood pellets. *Fuel Process. Technol.* **129**(129), 168–173 (2015)
24. Kaliyan, N., Morey, R.V.: Densification characteristics of corn stover and switchgrass. *Trans. ASABE* **52**(3), 907–920 (2009)
25. Jiang, L.B., Liang, J., Yuan, X.Z., Li, H., Li, C.Z., Xiao, Z.H., Huang, H.J., Wang, H., Zeng, G.M.: Co-pelletization of sewage sludge and biomass: the density and hardness of pellet. *Biores. Technol.* **166**(8), 435–443 (2014)
26. Peng, J.H., Bi, X.T., Sokhansanj, S., Lim, C.J.: Torrefaction and densification of different species of softwood residues. *Fuel* **111**, 411–421 (2013)
27. Stelte, W., Holm, J.K., Sanadi, A.R., Barsberg, S., Ahrenfeldt, J., Henriksen, U.B.: Fuel pellets from biomass: the importance of the pelletizing pressure and its dependency on the processing conditions. *Fuel* **90**(11), 3285–3290 (2011)
28. Li, H., Liu, X.H., Legros, R., Bi, X.T., Lim, J., Sokhansanj, S.: Pelletization of torrefied sawdust and properties of torrefied pellets. *Appl. Energy* **93**, 680–685 (2012)
29. Kong, L.J., Tian, S.H., He, C., Du, C.M., Tu, Y.T., Xiong, Y.: Effect of waste wrapping paper fiber as a “solid bridge” on physical characteristics of biomass pellets made from wood sawdust. *Appl. Energy* **98**, 33–39 (2012)
30. Jiang, L.B., Yuan, X.Z., Xiao, Z.H., Liang, J., Li, H., Cao, L., Wang, H., Chen, X.H., Zeng, G.M.: A comparative study of biomass pellet and biomass-sludge mixed pellet: energy input and pellet properties. *Energy Convers. Manage.* **126**, 509–515 (2016)
31. Kong, L.J., Xiong, Y., Liu, T., Tu, Y.T., Tian, S.H., Sun, L.P., Chen, T.: Effect of fiber natures on the formation of “solid bridge” for preparing wood sawdust derived biomass pellet fuel. *Fuel Process. Technol.* **144**, 79–84 (2016)